

Study of the behavior of an instrumented soil nail wall in Salvador-Brazil

André Luiz Delmondes Filho^{1#} , Erinaldo Hilário Cavalcante² ,
Carlos Rezende Cardoso Júnior² , Demóstenes de Araújo Cavalcanti Júnior² 

Article

Keywords

Soil nailing
Numerical modeling
Displacement monitoring
Instrumentation

Abstract

This paper aims to analyze the behavior of a soil-nailed excavation located in Salvador, Bahia, Brazil. Numerical stress-strain modeling was conducted, using finite element method. The horizontal displacement profiles obtained for the wall face in the numerical analysis presented a good correlation compared to field instrumentation monitoring with inclinometers. The results showed that the magnitude of the maximum numerical and experimental displacements was lower than the simplified models recommended by international manuals and technical literature. However, the monitoring data was compatible with other cases of instrumented nailed excavations in silt-sandy soil in the city of Salvador. Numerical models also adequately represented the distribution of tensile forces in nails. The maximum tensile forces observed numerically were smaller than those calculated using analytical methods. It was emphasized that the results of field monitoring and numerical models correspond to a stage immediately after the end of the retaining structure execution, not considering the evolution of deformations in long term.

1. Introduction

Soil nailing is a widely used technique to stabilize cut slopes in Brazil. In the Brazilian practice of soil nailing design, the stability analysis is normally based on limit equilibrium methods, i.e., in obtaining a safety factor for the evaluated sliding surfaces. However, this methodology does not predict the deformations in the reinforced soil mass and, consequently, does not accurately represent the behavior of the structure, whereas the stress redistribution in nails is not considered.

In addition to theoretical analysis in the design phase, soil nail performance evaluation has proved to be of fundamental importance, using instrumentation and field tests, both during the construction and utilization phases. This routine is also included in the recent Brazilian standard NBR 16920-2 (ABNT, 2021). By this framework, this work aims to analyze the behavior of a soil-nailed excavation using numerical analysis, based on the interpretation of monitoring data and other tests performed, for a case study in Salvador, Bahia, Brazil.

2. Background on soil nail wall displacements and internal forces

In the initial context, several instrumentation programs performed in nailed structures had contributed to the definition

of displacements magnitude in nailed soil walls and reported that horizontal displacements at the top of the excavation present values between 0.1 and 0.5% of its height (H), at the end of the construction phase (e.g. Clouterre, 1991; Gaessler & Gudehus, 1981; Mitchell & Villet, 1987). Based on these results, some international manuals (e.g. Clouterre, 1991; Lazarte et al., 2015) propose simplified formulas for maximum horizontal displacement on the top of the wall, equal 0.002H to 0.003H, depending on sandy or clayey soils, respectively.

According to Yuan et al. (2019b), the main simplified models for wall displacement prediction only take wall height and soil type into account, disregarding wall geometry, nail length, spacing and inclination angle, and external surcharge loading influence. Furthermore, the effect of time on displacement magnitude is also not considered. Data from monitored structures indicate that displacements in nailed soils tend to increase post-construction, especially in the first six months, depending on the type of soil, and may increase up to 15% in long term (Lazarte et al., 2015).

Over the last decades, numerical methods have been one of the main tools for predicting deformations in nailed soil masses, especially using the finite element method (FEM), both 2D and 3D analysis. The numerical tools are capable of simulating constructive phases and incorporating constitutive models, which reproduce the structure behavior with certain

#Corresponding author. E-mail address: delmondes@usp.br

¹Universidade de São Paulo, Escola Politécnica, São Paulo, São Paulo, SP, Brasil.

²Universidade Federal de Sergipe, Departamento de Engenharia Civil, São Cristóvão, SE, Brasil.

Submitted on October 25, 2021; Final Acceptance on September 5, 2022; Discussions open until February 28, 2023.

<https://doi.org/10.28927/SR.2022.076221>



This is an Open Access article distributed under the terms of the Creative Commons Attribution License, which permits unrestricted use, distribution, and reproduction in any medium, provided the original work is properly cited.

fidelity, in static, seismic, or dynamic conditions (e.g. Garzón-Roca et al., 2019; Gerscovich et al., 2005; Lima, 2002; Razavi & Hajjalilue Bonab, 2017; Sharma & Ramkrishnan, 2020). Recently, some studies have applied statistical approaches and machine learning techniques, including artificial neural network (ANN) for nailed wall displacement prediction (e.g. Liu et al., 2021; Yuan et al., 2019b).

Regarding soil nail monitoring, the investigation conducted by Saré (2007) showed that instrumentation with inclinometers is efficient both for obtaining point displacements and for assessing the global displacement of the soil mass. The comparison between the data obtained by the field monitoring and the results of the numerical analysis was satisfactory regarding the prediction of the retaining structure displacements and the loads acting in the nails. Other technologies also successfully applied for soil nail monitoring include Brillouin distributed optical fiber sensors (DOFS), Fiber Bragg grating (FBG) sensors, and unmanned aerial vehicles (UAV) (Esmacili et al., 2019; Hong et al., 2017; Hu et al., 2018).

The geometric line with the maximum axial tensile force in the nails could define a potential rupture surface, which separates the soil mass into two zones: the active zone and the passive zone (Ehrlich, 2003). In the nailed excavations instrumented and monitored by Clouterre (1991), the distance between the face of the retaining wall and the line of maximum tension in the nails presented values between 0.3 and 0.5 times the excavation height (H). Lazarte et al. (2015) indicate that this value can be between $0.3H$ and $0.4H$ for the upper nails and between $0.15H$ and $0.20H$ for the lower ones (Figure 1).

Some approaches and formulations have been proposed to estimate the maximum tensile force (T_{max}) acting in the nails, as a function of the active earth pressure coefficient (K_a), the soil unit weight (γ), the excavation height (H), and the horizontal (S_h) and vertical (S_v) spacing between nails

(Briaud & Lim, 1997; Lazarte, 2011; Lazarte et al., 2015; Lin et al., 2017; Lin & Bathurst, 2018; Yuan et al., 2019a). Briaud & Lim (1997) propose Equations 1 and 2 for the upper nail line and the lower ones, respectively. Lazarte et al. (2015) provided expressions 3 and 4, for nails located at the upper two-thirds and the lower third of the excavation, respectively.

$$T_{max} = 0.65 \times K_a \times \gamma \times H \times S_v \times S_h \quad (1)$$

$$T_{max} = 0.33 \times K_a \times \gamma \times H \times S_v \times S_h \quad (2)$$

$$T_{max} = 0.75 \times K_a \times \gamma \times H \times S_v \times S_h \quad (3)$$

$$T_{max} = 0.38 \times K_a \times \gamma \times H \times S_v \times S_h \quad (4)$$

3. Case study of a nailed wall in Salvador, Brazil

3.1. Project description, geotechnical characterization and field instrumentation

The soil-nailed wall under study is part of a residential project in Salvador, Bahia, Brazil. The necessary data for this work were obtained from the company responsible for the retaining system design. Figure 2 shows two photographic records of the structure during its construction phase.

The retaining structure presents heights between 7.7 and 14.8 meters. The project used different configurations for nail length: 6.0 and 12.0 m (e.g. sections E 2+10.00 and E 4+0.00) and 6.0, 9.0, and 12.0 m (e.g. E 3+10.00). Nails were composed of steel bars of 20 mm in diameter, type CA-50, and drilling hole diameter equal to 75 mm. The excavated site is composed, basically, of interleaved layers of sandy silt and clay silt with sand, as illustrated in the geotechnical cross-view in Figure 3.

The field instrumentation of the nailed excavation included inclinometers for monitoring horizontal displacements in the nailed wall. Four inclinometers were inserted at different stations according to Table 1 and the soil nailed wall was monitored until the end of the construction phase. The location of the inclinometers is illustrated in Figure 4. A qualitative analysis of the monitoring data was conducted and verified a good profile of Inclinometer 1, which was defined as the reference values for the present study.

Table 1. Summary of installed inclinometers for the soil nailed wall case.

Inclinometer N°	Location/Station	Depth (m)
1	E 2+10,00	22.5
2	E 5+10,00	22.5
3	E 8+0,00	15.5
4	E 7+0,00	21.5

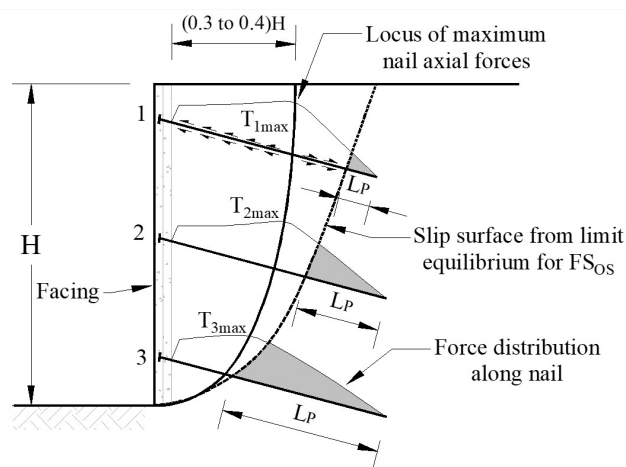


Figure 1. Position of the potential rupture surface and locus of maximum nail axial forces (Lazarte et al., 2015).

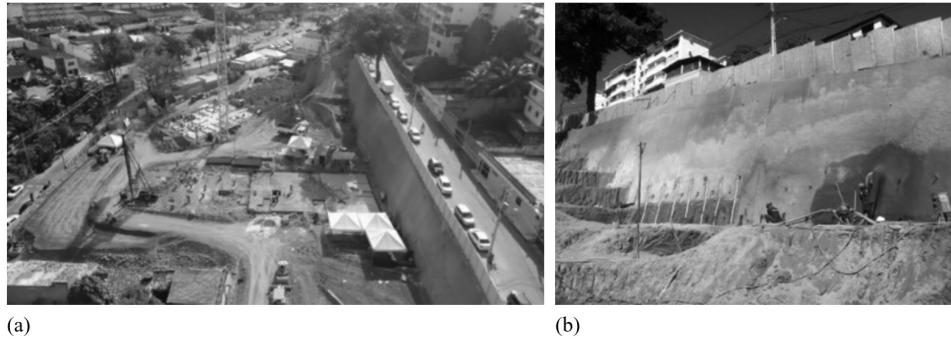


Figure 2. Construction of the soil-nailed wall. Top view (a) and front view (b), during shotcrete application stage.

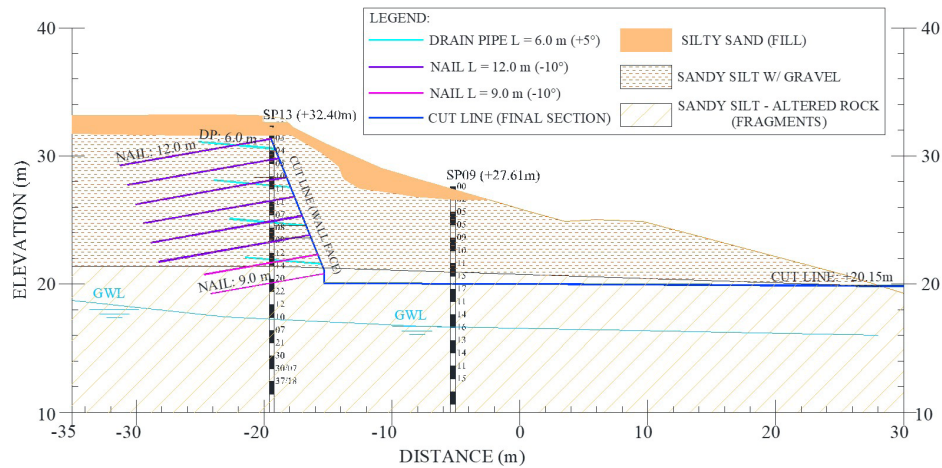


Figure 3. Geotechnical cross-view – Section E 3+10.00.

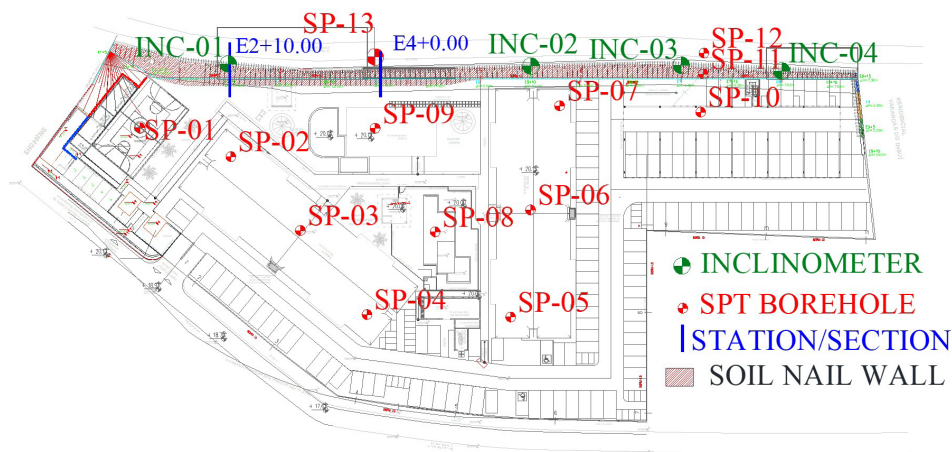


Figure 4. Location of reference sections, inclinometers, and Standard Penetration Tests performed on-site.

3.2. Numerical modeling procedure

The numerical analysis was conducted using the finite element method software SIGMA/W, as a module GeoStudio 2012 geotechnical package. Two cross-sections were analyzed, E 2+10.00 and E 4+0.00. As presented in Table 1,

section E 2+10.00 was instrumented with an inclinometer and monitored until the end of the construction phase. Thus, the analysis of this section was conducted to calibrate the soil deformability parameters, comparing the displacements obtained in the numerical model with the ones obtained by the field monitoring.

Geometry inserted for analysis of section E 2+10.00 in the initial condition (*InSitu*) is presented in Figure 5a. The sub-horizontal lines represent the nails, while the vertical one reproduces the inclinometer installed in the section. To simplify the model, only two layers of soil were adopted (see legend). On the right side of the reinforced area, the division of layers aims to represent the excavation stages. The sequential steps of excavation and insertion of the nails were reproduced in the model, for each reinforcement level, to represent the stress changes in the soil. The final condition of the analysis is illustrated in Figure 5b.

The finite element mesh was generated using quadrilateral and triangular elements with a global dimension equal to

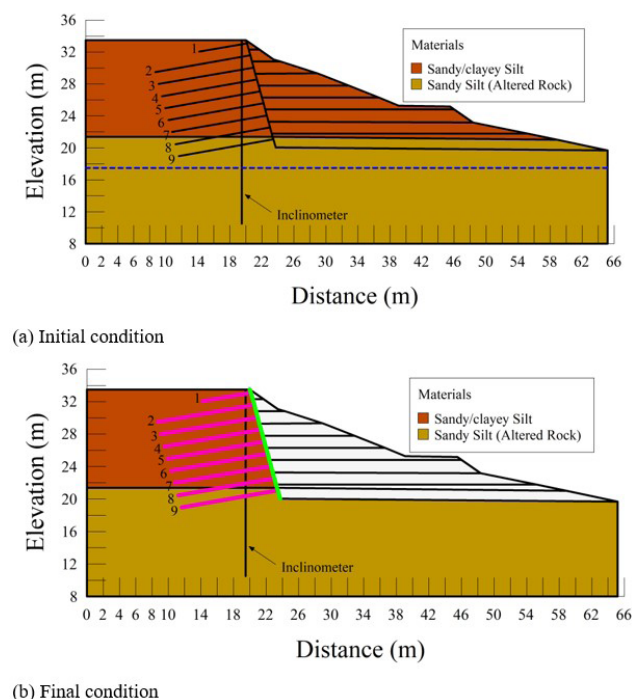


Figure 5. Model of section E 2+10.00, in initial (a) and final (b) conditions.

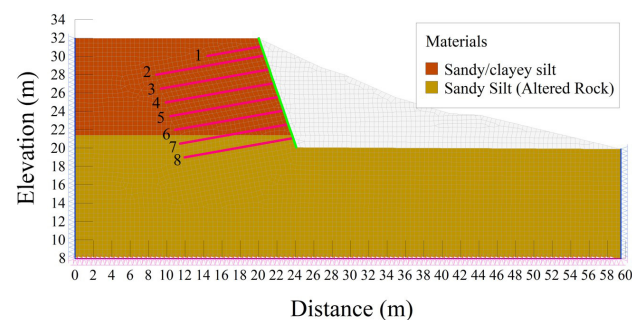


Figure 6. Final model of E 4+0.00 section, including mesh and boundary conditions.

0.50 m, a value suggested by Corte (2017), who also performed numerical and stability simulations in nailed soil using the GeoStudio software. The mesh of the model in section E 4+0.00 was composed of 4949 elements, totaling 5050 nodes. This unstructured quadrilateral and triangular mixed mesh is recommended for general cases in excavation analysis (GEO-SLOPE, 2013). The geometry inserted for the model of section E 4+0.00 in the final condition of excavation is presented in Figure 6.

The pink and green lines in the models correspond, respectively, to the nails and the shotcrete facing, inserted in the model as beam elements. Nails were modeled with a design inclination equal to 10° and lengths of 6.0 and 12.0 m (according to the design of each section), for both analyzed sections. Connection between nail heads and shotcrete face was modeled as rigid. The necessary input data for the beam elements are cross-sectional area, moment of inertia, and Young's modulus.

Geometric parameters were calculated according to the design specifications. The model used the nails' equivalent moment of inertia, considering the horizontal spacing, for an adequate representation of the elements bending stiffness. The Young's modulus (E_{beam}) applied to the beam elements was calculated according to the weighted average of steel and concrete areas (in the case of the nails, the grout material). This procedure was used in the numerical simulations performed by Gerscovich et al. (2005) and by Singh & Babu (2010). A synthesis of the geometric and elastic parameters applied in beam elements of the nails and the coating (wall face) is presented in Table 2, as input data in the software.

Soil was represented by the elastic-plastic model with Mohr-Coulomb rupture criteria, for which, in addition to the unit weight (γ), five other parameters are needed: Young's modulus (E_{soil}), internal friction angle (ϕ), cohesion (c), dilatancy angle (ψ) and Poisson's ratio (ν). The Young's modulus of the soil layers was obtained by adjusting the displacements of the model with those monitored in the field, for the instrumented section E 2+10.00. The values of 35 and 48 MPa for the upper and lower layers, respectively, were those that led to the best approximation between the displacements of the numerical model and those measured by the inclinometer. The shear strength parameters were obtained from direct shear tests, except the dilatancy angle, which was adopted null, following the recommendations of the SIGMA/W manual (GEO-SLOPE, 2013). The analyses carried out by Pereira (2016) also followed this recommendation. Poisson's ratio was adopted 0.25, according to the suggested range of values

Table 2. Elastic and geometric parameters of the beam elements used in numerical models.

Element	Young's modulus (GPa)	Area (cm ²)	Inertia (cm ⁴)
Nail	34.4	44.2	155.3
Wall face	24.1	800	4266.7

for sandy soils in Jia (2018). Table 3 presents a synthesis of the soil parameters applied in the analyses for both sections.

4. Analysis results and discussion

4.1. Wall displacements

A map of horizontal displacements in the entire model analyzed for section E 2+10.00 is shown in Figure 7. The horizontal displacements on the nailed soil wall face range from 2.5 to 4.5 mm, with greater values at the top of the retaining structure. For section E 4+0.00, the same map is

shown in Figure 8. For this section, horizontal displacements on the face of the nailed soil range from 1.5 to 3.0 mm, with higher values also in the vicinity of the retainer's top.

The horizontal displacement profile on the excavation face of section E 2+10.00 is illustrated in Figure 9a, for all excavation phases. Reinforcing what was seen in Figure 7, in the curves, the maximum displacement equal to 4.7 mm is found at the top of the structure. However, in the lower third of the excavation, displacements reaching values of 4.0 mm are observed. The significant displacement values in the lower third of the excavation can be simply associated with the efforts resulting from lateral earth pressure, which is higher in that area. Another aspect that calls attention is the evolution of displacements with the advance of the excavation phases. For this section, in the last three stages, the maximum displacement at the top has increased by 88%, going from 2.5 mm (end of Step 6) to 4.7 mm (Step 9, final). Also, for section E 2+10.00, Figure 9b shows the curves of the horizontal displacements obtained by the numerical model for the vertical line, inserted to represent the inclinometer

Table 3. Elastic and geometric parameters of the beam elements.

Soil description	γ (kN/m ³)	E_{soil} (MPa)	Φ (°)	c (kPa)	ψ (°)	ν
Sandy/silty clay	16.7	35	28.7	16.5	0	0.25
Sandy silt (altered rock)	17.0	48	24.5	25.0	0	0.25

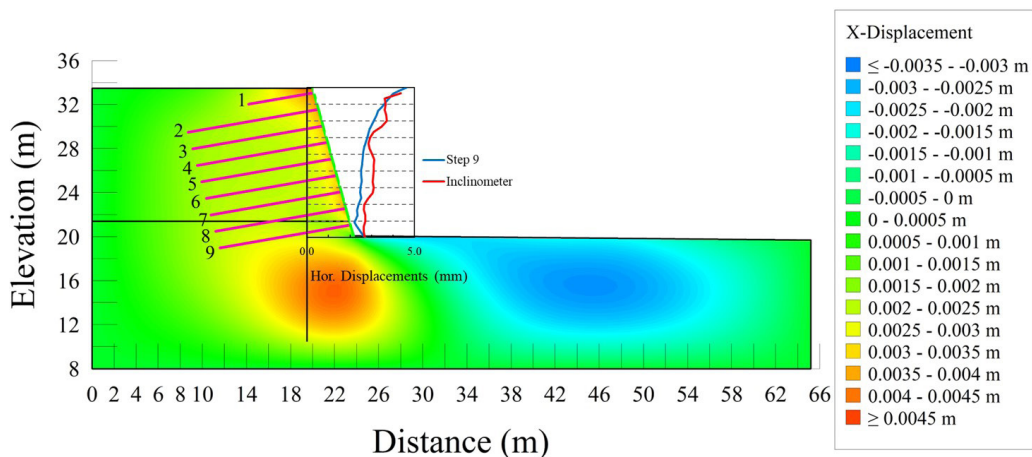


Figure 7. Section E 2+10.00. Horizontal displacements (in X) – Final step.

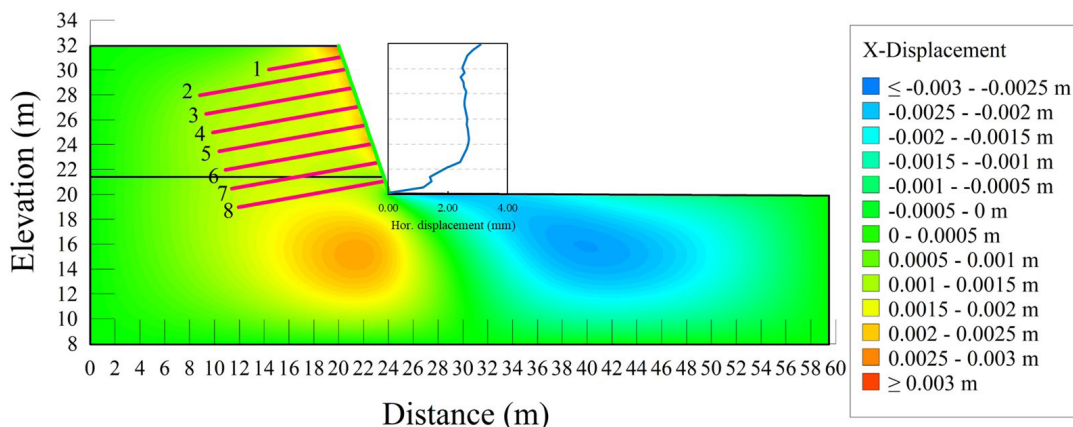


Figure 8. Section E 4+0.00. Horizontal displacements (in X) – Final step.

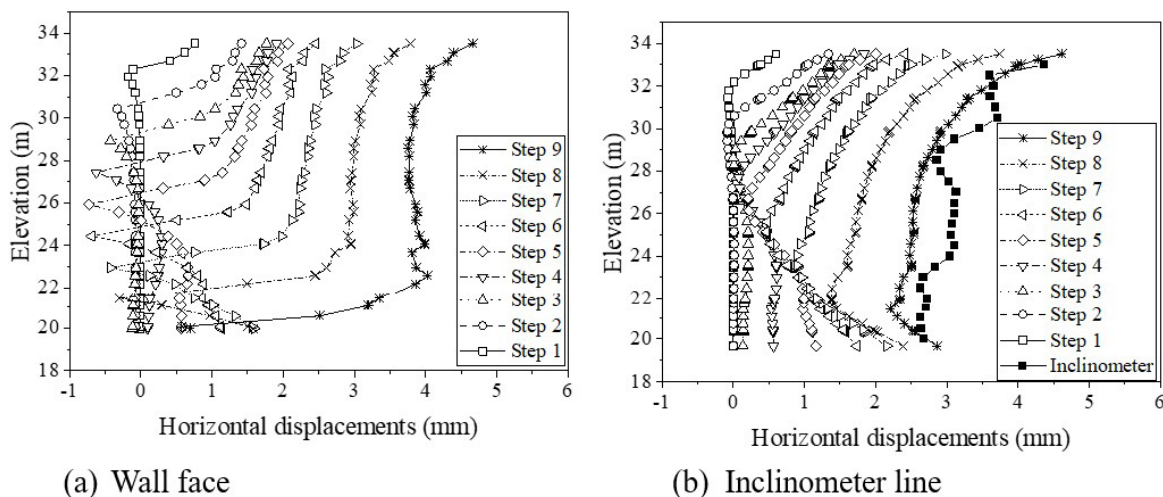


Figure 9. Horizontal displacement profiles (in X) for section E 2+10.00. (a) Wall face; (b) Inclinator line.

installed in the field, as well as the horizontal displacements obtained by the real inclinometer. The figure shows a good correlation between the results obtained from the numerical analysis and the values obtained from the readings performed with the inclinometer, with the excavation completed, for the adopted elastic parameters.

The horizontal displacement profile on the excavation face of section E 4+0.00 is illustrated in Figure 10, for all excavation phases. Again, in the curves, the maximum displacements were found at the top, reaching 3.1 mm in the final stage. In the lower half of the excavation, for the final step, maximum displacements of 2.7 mm are observed. As in the analysis of section E 2+10.00, it can be reiterated the evolution of displacements with the advance of excavation phases. In the last three phases, the displacements at the top more than doubled in value, increasing from 1.4 mm (end of Step 5) to 3.1 mm (Step 8, final).

Analyzing the results of the two modeled sections, the displacement profiles showed similar behavior, with maximum horizontal displacements at the top. However, considerable displacements were also found in the bottom half of the excavation. This behavior has been discussed in some studies, such as Cardoso & Carreto (1989), Barley (1992), Shiu et al. (1997), and Lima (2002), who report the influence of the excavation face inclination on the horizontal displacement profile, since the analytical predictions more widespread by the technical literature are valid for vertical excavations (90°), differently from the model of this research. In some cases, for smaller slopes, maximum displacements even tend to be located below the top.

Regarding the magnitude of horizontal displacements, for both analyzed sections, the maximum values are in the order of 0.03% of the excavation height. This result is considerably smaller than the predictions made by international literature. However, a study of the behavior of nailed excavations performed in Salvador, Brazil, by

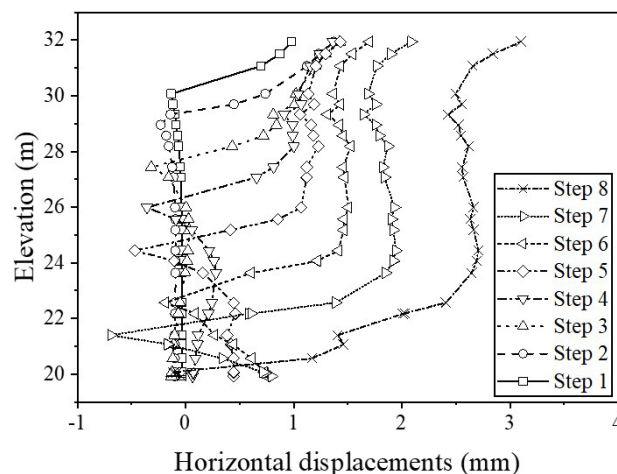


Figure 10. Horizontal displacement profile (in X) for section E 4+0.00.

Décourt et al. (2003), also showed results much smaller than the analytical predictions. The maximum displacements obtained by the authors, also in silty-sandy soil, were in the order of 0.07% of the excavation height. In this context, it should be noted that both the results of field monitoring and those obtained from numerical models correspond to a stage immediately after the end of the retaining structure execution, not considering the evolution of the deformations over time, that is, in the long term.

4.2. Axial load distribution on nails

The distribution of the axial tensile load along the nails length (L_{nail}) for section E 2+10.00, referring to the end of the construction, is shown in Figure 11 a. The graph is presented in a way that the nail length axis starts on the right, corresponding to the face of the wall (head of the nails), in order to represent

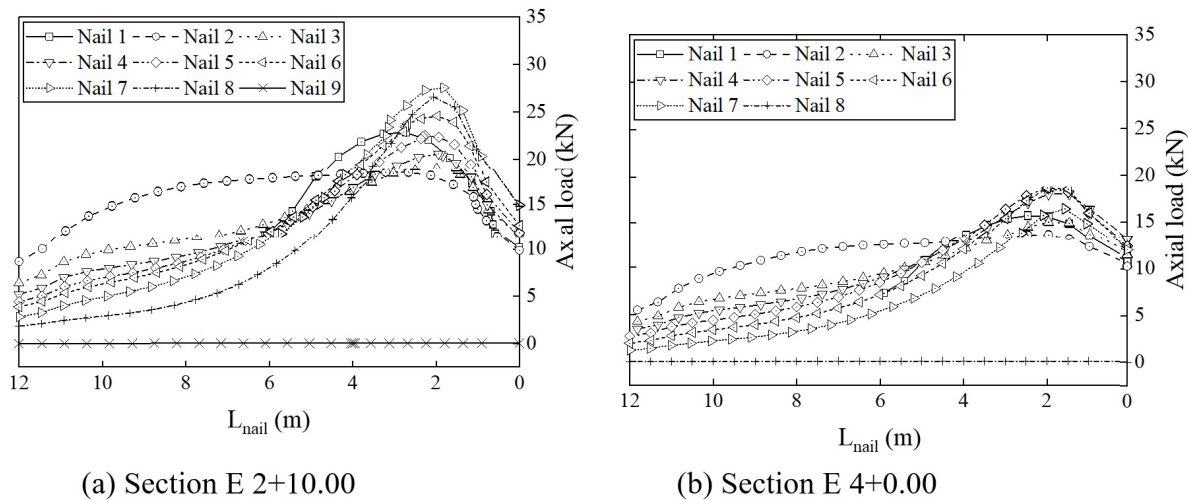


Figure 11. Distribution of axial tensile load along the nails length after the excavation is completed. (a) Section E 2+10.00; (b) Section E 4+0.00.

the position of the reinforcements in the models. For this section, the maximum forces in the nails varied between 18 kN (nail 2) and 28 kN (nail 7). It is noteworthy that the loads obtained for the lower nail line (nail 9) were practically null. Figure 11b shows the distribution of the axial tensile load along the nails' length in section E 4+0.00, referring to the end of the execution. For this section, the maximum forces in the nails varied between 14 kN (nail 2) and 18 kN (nail 6). Similarly, to section E 2+10.00, the loads obtained for the lowest nail line (nail 8) were practically null.

For both sections, a similar distribution of tensile force is observed, in which the maximum loads are located at a distance from the wall face that corresponds to values of $0.14H$ and $0.17H$. Predictions made by Clouterre (1991) indicate that the maximum load line can be placed at a distance of $0.30H$ to $0.50H$. In Lazarte et al. (2015) this value varies between $0.30H$ and $0.40H$, for nails closer to the top, and between $0.15H$ and $0.20H$ for the lower nail lines. Regarding the maximum tensile forces, the values obtained in the two num

erical analyses are considerably smaller than those predicted using the methodologies proposed by Briaud & Lim (1997) and by Lazarte et al. (2015), which provide values from 50 to 130 kN, considering the different positions of the nails. However, it is significant that both proposals cited do not consider the effect of cohesion, and do not represent well the soil under study. If cohesion were considered mathematically in the distribution of the active earth pressure acting on the nails, perhaps the authors' proposals would approximate the results obtained in the numerical analyses. Similar observations are presented by Santos (2019) and Ehrlich et al. (2021).

The relation between the tensile force close to the wall face (nail head) and the maximum tensile force in the

nails presented an average value of 0.54 and 0.68 for the sections E 2+10.00 and E 4+0.00, respectively, approaching Clouterre's analytical predictions (Clouterre, 1991). It's also possible to observe relatively small load values at the end of the nails, except for nail 2, positioned in the higher portion of the excavation, which was possibly influenced by the shorter nail 1 (first line), as discussed in Razavi & Hajjalilue Bonab (2017).

5. Conclusions

This paper presented the analysis of the behavior of a soil-nailed excavation carried out in the city of Salvador, Bahia, Brazil. Some constraints on the retaining structure behavior were evaluated, related to deformations and stress on the nails:

- The horizontal displacement profiles from the numerical models and the inclinometer monitoring showed very similar behavior. The displacements observed in numerical models for two sections analyzed in this work were equivalent, with maximum horizontal displacements at the top, but with significant values in the lower portion of the excavation;
- Regarding the magnitude of the horizontal displacements, the maximum values obtained were of the order of 0.03% of the excavation height (H), therefore, smaller than the predictions of the international literature ($0.002H$ to $0.003H$) but compatible with other cases of instrumented nailed excavations in silt-sandy soil in the city of Salvador, as detailed in Décourt et al. (2003);
- The distribution of tensile forces in the nails was compatible with the analytical calculations, in which the maximum forces are located behind the face of the wall. However, the magnitude of the maximum

tensile forces was considerably smaller than the estimated by international manuals models. The relationship between the tensile force close to the face and the maximum tensile force in the nails, on the other hand, approached Clouterre's analytical predictions (Clouterre, 1991).

Acknowledgements

The authors acknowledge the Universidade Federal de Sergipe and GEOTEC Consultoria e Serviços Ltda. for the technical support given to this research, and the Brazilian agency Coordenação de Aperfeiçoamento de Pessoal de Nível Superior (CAPES) for the financial support provided to the first author during this study.

Declaration of interest

The authors have no conflicts of interest to declare.

Authors' contributions

André Luiz Delmondes Filho: conceptualization, data curation, formal analysis, methodology, visualization, writing – original draft. Erinaldo Hilário Cavalcante: conceptualization, methodology, project administration, resources, supervision, validation. Carlos Rezende Cardoso Júnior: conceptualization, investigation, methodology, resources, supervision. Demóstenes de Araújo Cavalcanti Júnior: conceptualization, investigation, resources.

List of symbols

c	Soil cohesion
E_{beam}	Young's modulus of beam elements (numerical analysis)
E_{soil}	Young's modulus of soil
H	Excavation depth
K_a	Active earth pressure coefficient
L_{nail}	Nail length
T_{max}	Maximum tensile force acting in the nails
S_h	Horizontal spacing between nails
S_v	Vertical spacing between nails
γ	Soil unit weight
ϕ	internal friction angle of soil
ν	Poisson's ratio of soil
ψ	Dilatancy angle

References

ABNT 16920-2. (2021). *Walls and Slopes in Reinforced Soils - Part 2: Soil Nail*. ABNT - Associação Brasileira de Normas Técnicas, Rio de Janeiro, RJ (in Portuguese).

- Barley, D.A. (1992). Soil nailing - case histories and developments. In: *Proceedings of the ICE Conference on Retaining Structures*, Cambridge.
- Briaud, J.-L., & Lim, Y. (1997). Soil-nailed wall under piled bridge abutment: simulation and guidelines. *Journal of Geotechnical and Geoenvironmental Engineering*, 123(11), 1043-1050. [http://dx.doi.org/10.1061/\(ASCE\)1090-0241\(1997\)123:11\(1043\)](http://dx.doi.org/10.1061/(ASCE)1090-0241(1997)123:11(1043)).
- Cardoso, A.S., & Carreto, A.P. (1989). Performance and analysis of a nailed excavation. In: *Proceedings of the 12th International Conference on Soil Mechanics and Foundation Engineering* (pp. 1233–1236). Rio de Janeiro. Publications Committee of XII ICSMFE.
- Clouterre. (1991). *Recommendations CLOUTERRE 1991. Soil Nailing Recommendations-1991 for Designing, Calculating, Constructing and Inspecting Earth Support Systems Using Soil Nailing*. U.S. Department of Transportation, Federal Highway Administration.
- Corte, F.H. (2017). *Containment analysis in nailed soil in the city of São Bernardo do Campo/SP* [Master's dissertation, Universidade Estadual de Campinas]. Universidade Estadual de Campinas' repository (in Portuguese). <https://doi.org/10.47749/T/UNICAMP.2017.989014>.
- Décourt, L., de Campos, L.E.P., & Menezes, M.S.S. (2003). Projeto e comportamento de escavações estabilizadas com solo grampeado em Salvador. In *Solo grampeado - Projeto, execução, instrumentação e comportamento - Workshop* (pp. 105-120). São Paulo, SP: ABMS.
- Ehrlich, M. (2003). Solos grampeados - Comportamento e procedimentos de análise. In *Solo grampeado - Projeto, execução, instrumentação e comportamento - Workshop* (pp. 127-137). São Paulo, SP: ABMS.
- Ehrlich, M., Rosa, C. A. B., & Mirmoradi, S. H. (2021). Effect of construction and design factors on the behaviour of nailed-soil structures. *Proceedings of the Institution of Civil Engineers - Geotechnical Engineering*, 1-13. <https://doi.org/10.1680/jgeen.20.00139>.
- Esmaeili, F., Ebadi, H., Saadatseresht, M., & Kalantary, F. (2019). Application of UAV photogrammetry in displacement measurement of the soil nail walls using local features and CPDA method. *ISPRS International Journal of Geo-Information*, 8(1), 25. <http://dx.doi.org/10.3390/ijgi8010025>.
- Gaessler, G., & Gudehus, G. (1981). Soil Nailing - Some Aspects of a New Technique. In: *Proceedings of the 10th International Conference on Soil Mechanics and Foundation Engineering*, Stockholm. (Vol. 3, pp. 665-670), Publications Committee of X ICSMFE.
- Garzón-Roca, J., Capa, V., Torrijo, F.J., & Company, J. (2019). Designing soil-nailed walls using the amherst wall considering problematic issues during execution and service life. *International Journal of Geomechanics*, 19(7), 05019006. [http://dx.doi.org/10.1061/\(ASCE\)GM.1943-5622.0001453](http://dx.doi.org/10.1061/(ASCE)GM.1943-5622.0001453).

- GEO-SLOPE. (2013). *Stress-deformation modeling with SIGMA/W - an engineering methodology*. GEO-SLOPE International Ltd.
- Gerscovich, D.M.S., Sieira, A.C.C.F., Lima, A.P., & Sayão, A.S.F.J. (2005). Técnicas de modelagem numérica de escavações de taludes em solo grampeado. In: *Proceedings of the IV Conferencia Brasileira sobre Estabilidade de Encostas*, (pp. 671-680). Salvador.
- Hong, C.Y., Zhang, Y.F., Li, G.W., Zhang, M.X., & Liu, Z.X. (2017). Recent progress of using Brillouin distributed fiber optic sensors for geotechnical health monitoring. *Sensors and Actuators. A, Physical*, 258, 131-145. <http://dx.doi.org/10.1016/j.sna.2017.03.017>.
- Hu, Y., Hong, C., Zhang, Y., & Li, G. (2018). A monitoring and warning system for expressway slopes using FBG sensing technology. *International Journal of Distributed Sensor Networks*, 14(5), 155014771877622. <http://dx.doi.org/10.1177/1550147718776228>.
- Jia, J. (2018). Soil dynamics and foundation modeling. In J. Jia (Ed.), *Soil dynamics and foundation modeling: offshore and earthquake engineering*. Springer. <https://doi.org/10.1007/978-3-319-40358-8>.
- Lazarte, C.A. (2011). *Proposed specifications for LRFD Soil-Nailing design and construction* (NCHRP Report 701). National Cooperative Highway Research Program.
- Lazarte, C.A., Robinson, H., Gómez, J.E., Baxter, A., Cadden, A., & Berg, R. (2015). Soil nail walls reference manual. In National Highway Institute. *Geotechnical Engineering Circular No. 7* (FHWA-NHI-14-007). U.S. Department of Transportation, Federal Highway Administration.
- Lima, A.P. (2002). *Deformability and stability of slopes supported by soil nailing* [Master's dissertation, Pontificia Universidade Católica do Rio de Janeiro - PUC-Rio]. PUC-Rio's repository (in Portuguese). <https://doi.org/10.17771/PUCRio.acad.3335>.
- Lin, P., & Bathurst, R.J. (2018). Reliability-based internal limit state analysis and design of soil nails using different load and resistance models. *Journal of Geotechnical and Geoenvironmental Engineering*, 144(5), 04018022. [http://dx.doi.org/10.1061/\(asce\)gt.1943-5606.0001862](http://dx.doi.org/10.1061/(asce)gt.1943-5606.0001862).
- Lin, P., Bathurst, R.J., & Liu, J. (2017). Statistical evaluation of the FHWA simplified method and modifications for predicting soil nail loads. *Journal of Geotechnical and Geoenvironmental Engineering*, 143(3), 04016107. [http://dx.doi.org/10.1061/\(asce\)gt.1943-5606.0001614](http://dx.doi.org/10.1061/(asce)gt.1943-5606.0001614).
- Liu, D., Lin, P., Zhao, C., & Qiu, J. (2021). Mapping horizontal displacement of soil nail walls using machine learning approaches. *Acta Geotechnica*, 16(12), 4027-4044. <http://dx.doi.org/10.1007/s11440-021-01345-z>.
- Mitchell, J.K., & Villet, W.C.B. (1987). *Reinforcement of earth slopes and embankments* (NCHRP Report 290). National Cooperative Highway Research Program.
- Pereira, A.B. (2016). *Estudos numéricos do comportamento tensão-deformação de estruturas em solo grampeado* [Master's dissertation, Universidade Federal de Ouro Preto]. Universidade Federal de Ouro Preto's repository (in Portuguese). <http://www.repositorio.ufop.br/handle/123456789/6532>
- Razavi, S.K., & Hajjalilue Bonab, M. (2017). Study of soil nailed wall under service loading condition. *Proceedings of the Institution of Civil Engineers - Geotechnical Engineering*, 170(2), 161-174. <http://dx.doi.org/10.1680/jgeen.16.00006>.
- Santos, C.A.B.R. (2019). *Numerical analysis of the behavior of soil nailing excavations: case study and influence of design and execution conditioners* [Master's dissertation, Universidade Federal do Rio de Janeiro]. UFRJ's repository (in Portuguese).
- Saré, A.R. (2007). *Behavior of an instrumented soil nailed excavation on a residual soil* [Doctoral thesis, Pontificia Universidade Católica do Rio de Janeiro - PUC-Rio]. PUC-Rio's repository (in Portuguese). <https://doi.org/10.17771/PUCRio.acad.11686>.
- Sharma, A., & Ramkrishnan, R. (2020). Parametric optimization and multi-regression analysis for soil nailing using numerical approaches. *Geotechnical and Geological Engineering*, 38(4), 3505-3523. <http://dx.doi.org/10.1007/s10706-020-01230-8>.
- Shiu, Y.K., Yung, P.C.Y., & Wong, C.K. (1997). Design, construction and performance of a soil nailed excavation in Hong Kong. In *Proceedings of the 14th International Conference on Soil Mechanics and Foundation Engineering* (pp. 1339-1342). Hamburg. Publications Committee of XIV ICSMFE.
- Singh, V.P., & Babu, G.L.S. (2010). 2D numerical simulations of soil nail walls. *Geotechnical and Geological Engineering*, 28(4), 299-309. <http://dx.doi.org/10.1007/s10706-009-9292-x>.
- Yuan, J., Lin, P., Huang, R., & Que, Y. (2019a). Statistical evaluation and calibration of two methods for predicting nail loads of soil nail walls in China. *Computers and Geotechnics*, 108, 269-279. <http://dx.doi.org/10.1016/j.compgeo.2018.12.028>.
- Yuan, J., Lin, P., Mei, G., & Hu, Y. (2019b). Statistical prediction of deformations of soil nail walls. *Computers and Geotechnics*, 115, 103168. <http://dx.doi.org/10.1016/j.compgeo.2019.103168>.